Climatology and trend analysis of global Total Columnar Ozone using OMI satellite data during 2004 -2017

Sateesh. M[1]* and Soni V. K[1].
[1]India Meteorological Department, New Delhi.

ABSTRACT

The depletion of ozone layer in the stratosphere changes the Earth's radiation budget and also causes human health effects. The ozone layer variation trend varies from location to location and drastic changes were found from equator to pole. In order to study the trend in the ozone layer OMI satellite L3 data on board Aqua has been utilized from 2004 to 2017 with 1^o X 1^o resolution data. The result shows the positive trend of 0.384 DU/year over the globe, whereas the Northern and Southern hemispheres are 0.499 DU/year, 0.383 DU/year. A highest positive recovery of 0.957 DU/year has been noticed over Antarctica region and an almost constant trend of 0.071 DU/year over Australia. A positive trend of 0.830 DU/year, 0.681 DU/year, 0.342 DU/year, 0.340 DU/year and 0.374 DU/year are noticed over North America, Asia, Europe, Africa and South America. Total Columnar Ozone (TCO) is high in the North Africa region. Highest depletion of ozone layer is found in 2007, 2012 and 2016 over Antarctica region and its depletion start at the end of the winter season. Nearly 300 DU TCO exists up to mid latitude and above 300 DU are in the high latitudes of Asia. Global mean value for the study period is 289.5 DU. The climatological values are 266.8 DU, 259.4 DU, 319.7 DU, 270 DU, 325 DU, 333.4 DU, 261.7 DU over Africa, Antarctica, Asia, Australia, Europe, North America and South America respectively. The climatological mean value over Northern hemisphere and Southern hemisphere are 294.4 DU and 275 DU respectively and the trends are 0.499, 0.383 respectively. Highest depletion of TCO is noticed in 2006 and 2015 early spring time over Antarctica.

KEYWORDS: Total Columnar Ozone, Ozone Monitoring Instrument, Climatology, TheilSen trend analysis.

Corresponding Author:
Mr. M. Sateesh
Senior Research Fellow,
Environment Monitoring and Research Division,
India Meteorological Department,
New Delhi – 110003.

1. INTRODUCTION

Global warming is become a serious concern in recent days due to the risks extreme weather events regionally and globally. There is a decreasing trend of surface temperatures from 1980 in the west Antarctica region (Soni et al., 2017).Ozone layer acts as a shield over the earth to protect from the harmful Ultraviolet rays (Norval et al., 2007). The depletion of ozone layer causes skin cancer and leads to global warming (Giannini, 1986). Ultraviolet rays radiation is the primary source for the production of ozone (O3) molecules and these ozone molecules continuously converted oxygen and back to ozone (Farman et al., 1985). The ground and observation shows a sharp decrease in total columnar ozone over Antarctica in the post winter and spring time in 1980s (Farman et al., 1985; Stolarski et al., 1986). The stable Chlorofluorocarbons do not break at the troposphere. When these CFCs drifted to stratosphere in the winter due to the strong vertex (Nash et al., 1996; Waugh, 1993) and interacted with the UV rays, the chlorine radical reacts with the ozone to produce ClO and O_2. This ClO again reacts with the O_3 to form two molecules of O_2 along with the free chlorine atom. This Cl atom will destroy thousands of ozone molecules until the Cl atom is removed from the stratosphere due to rain (James, G., 1986). The dynamics of polar vertex and its lower temperatures to form polar stratospheric clouds (PSCs) are the key ingredient to the depletion of ozone (Schoeberl and Hartmann, 1991). The aircraft measurement during the ozone hole period wind speeds may cross 100 $m.s^{-1}$ at the PSCs and above (Proffitt et al., 1990; Schoeberl and Hartmann, 1991) and the temperature are low as -88 ^{o}C and stay for long period until the break of PSCs.

A seven years (1979-1985) measurement of Solar Back scattering Ultraviolet (SBUV) instrument and Total Ozone Mapping Spectrometer (TOMS) on board Nimbus 7, a sun synchronous obtained a 40 % decrease of the columnar ozone concentration during the October month (Stolarski et al., 1986). There is a good agreement with the ground based observations with the OMI satellite observations with $r^2 > 0.8 – 0.9$ for various station observations (Balis et al., 2007; Herman et al., 2015; Kuttippurath et al., 2013; Liu et al., 2010; Vaz Peres et al., 2017). A recovery of ozone loss is +1 % during the 2000 to 2010 is observed where as -4 % of loss in 1979 to 1999 (Kuttippurath et al., 2013) over Antarctica.

The present study is about the spatial, temporal variation of total columnar ozone measured by the OMI satellite on board Aqua (Levelt et al., 2017, 2006; McPeters et al., 2015) and the recovery of ozone hole and its rate over the continents.

2. DATA AND METHODOLOGY

2.1 Ozone Monitoring Instrument (OMI)

The Ozone Monitoring Instrument (OMI) is a contribution of the Netherlands Agency for Aerospace Programs (NIVR) in collaboration with Finnish Meteorological Institute (FMI) to the National Aeronautics and Space Administration's (NASA) Aura mission and is orbiting the Earth on the Aura spacecraft. Aura satellite is part of NASA's Earth Observing System (EOS) long term mission and was launched in July 2004 from Vandenberg Air Force base in California into a polar sun-synchronous orbit (Levelt et al., 2006). The OMTO3 level 3 DOAS algorithm (Veefkind et al., 2003) gridded ozone data is collected from the site TCO data is collected from the ftp://toms.gsfc.nasa.gov/pub/omi/data/ozone/ site from October 2004 to April 2017. These daily data sets are averaged spatially, temporally according to the continental area by masking and then TheilSen trend (Sen, 1968; Theil, 1950) are calculated by considering bootstrap uncertainties.

3 Results and Discussions

3.1 TCO Climatology

The climatological mean of Total Columnar Ozone (TCO) is shown in Figure 3. the TCO values are more in the northern hemisphere as compared to the southern hemisphere. The TCO values are reaching to a maximum of 380 DU in the northern hemisphere and a low of 220 DU in the southern hemisphere and equatorial region. The seasonal variation of TCO is shown in Figure 4. Highest TCO concentrations are found in Northern hemisphere of winter season, and post winter season of the Southern hemisphere. Due to the presence of CFCs in the low temperature PSCs in over Antarctica region, ozone depletion is started in the early spring season to the polar vertex breaking period.

TCO concentrations are high in the Northern Hemisphere as compared to the Southern Hemisphere. And lowest TCO concentrations are at Antarctica region and followed by the tropical region. A positive trend of 0.384 DU/year is noticed over globally during the study period (Figure 1). The highest TCO concentrations are high in the April, May months due to the direct sun rays over the Northern Hemisphere and lowest TCO values are in the December month (Figure 2).

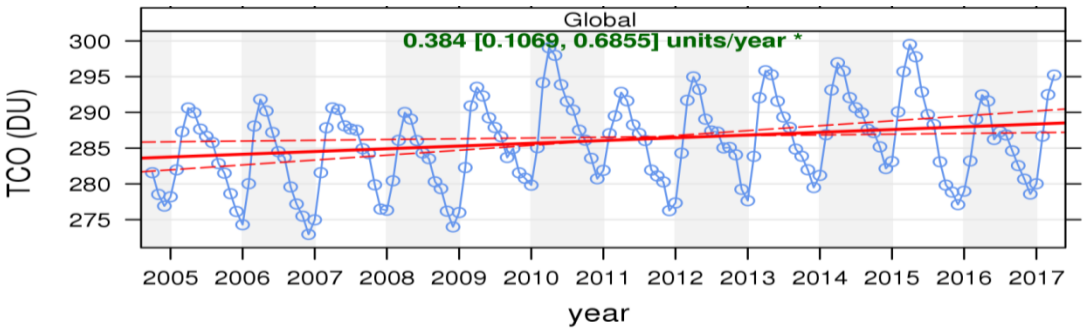

Figure 1: Mean TCO Theilsen trend line globally.

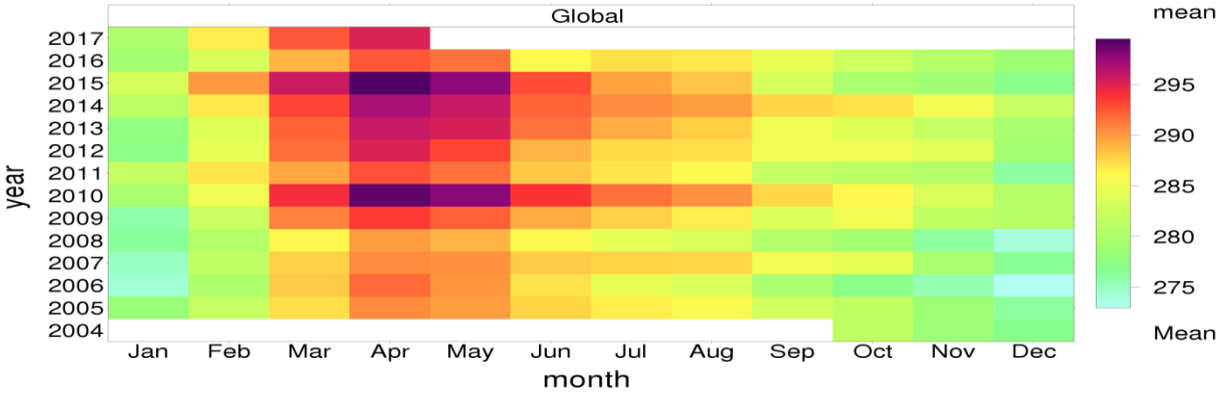

Figure 2: Heat map of Monthly means of TCO Globally.

Table1: Continental TCO monthly Averages; red color box indicates the maximum value and the green color indicates the minimum value.

	Jan	Feb	Mar	Apr	May	Jun	Jul	Aug	Sep	Oct	Nov	Dec
Africa	256.4	259.5	264.9	268.8	269.7	271.6	273.3	274.2	274.6	269.9	263.7	257.2
Arctic	277.5	268.9	267.2	278.5	290.4	306.2	309.6	251.1	182.9	179.0	233.8	276.2
Asia	328.9	358.7	359.0	359.0	343.3	319.3	298.7	290.6	288.0	291.2	294.7	304.7
Australia	257.3	255.9	255.7	257.4	260.3	267.8	271.6	280.2	289.9	291.7	284.9	269.6
Europe	336.1	355.6	372.3	373.7	357.9	336.4	318.6	302.1	289.6	279.3	285.9	304.3
N-America	341.6	374.4	388.3	382.3	359.6	334.8	314.5	298.6	289.8	292.4	305.0	317.7
S- America	252.8	251.7	253.4	252.6	252.6	259.2	266.2	273.8	278.2	274.9	267.3	258.6
Northern Hemisphere	288.6	304.3	316.7	320.8	314.4	302.9	293.4	286.4	280.8	275.8	273.9	277.3
Southern Hemisphere	269.1	264.9	264.2	264.9	267.2	272.2	280.5	287.1	286.5	288.8	285.5	277.5
Global	278.4	284.0	290.6	294.0	292.9	289.3	287.8	286.9	283.8	282.6	280.3	277.7

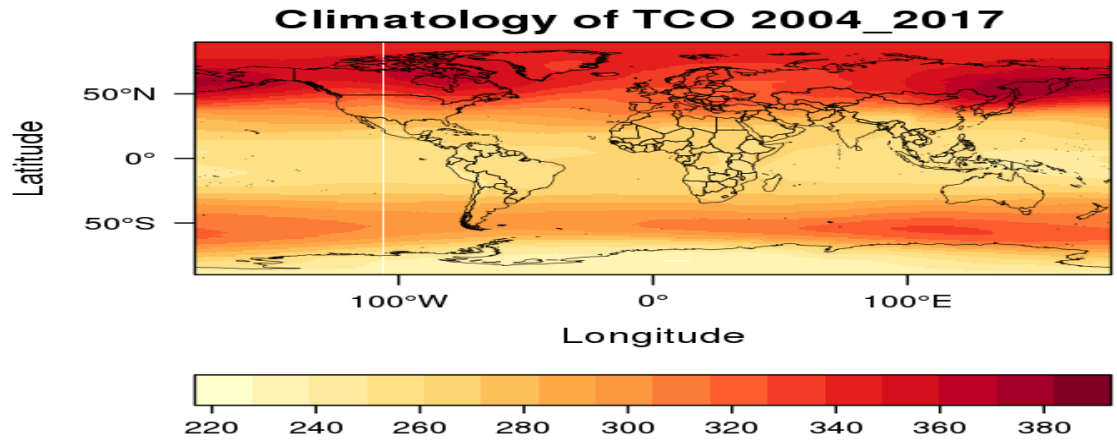

Figure 3: Climatological mean of Total Columnar Ozone from 2005 to 2016 using OMI satellite.

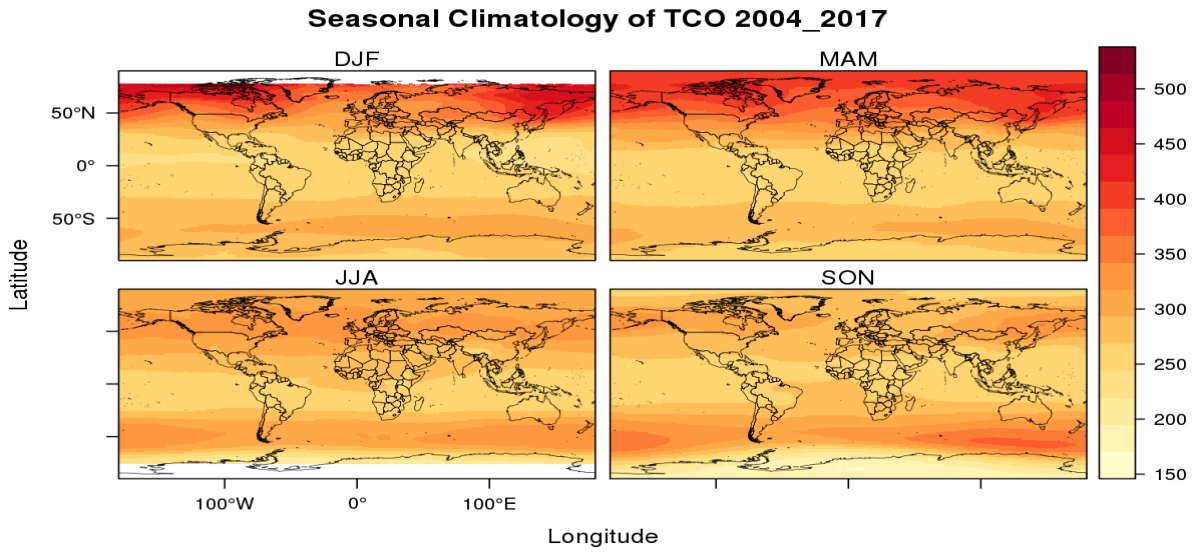

Figure 4: Climatological seasonal mean of Total Columnar Ozone from 2004 to 2017 using OMI satellite.

3.2 Continental wise analysis

3.2.1 Africa

The highest TCO concentrations are found in August and September months, lowest values are found in December, January months. Lowest TCO values are observed in 2006, 2010 and 2013 over Africa (Figure 6). The spatial Climatological plot shows high TCO concentrations are at Northern parts of Africa and lowest values are found at Southern part of South Africa (Figure 3). There is a positive trend of 0.34 DU/year noticed during the study period.

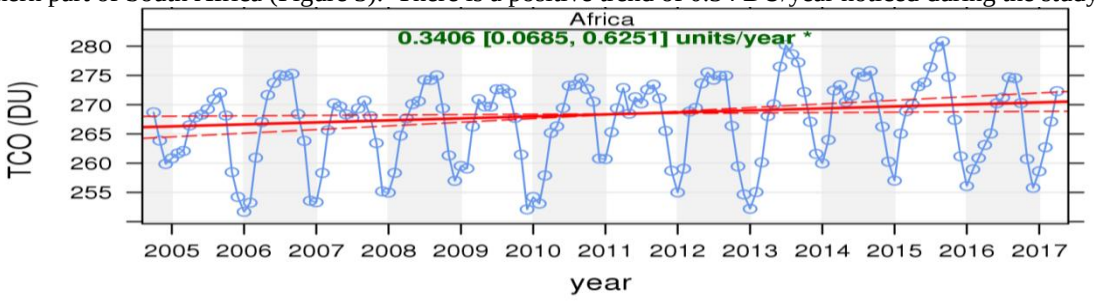

Figure 5: Mean TCO Theilsen trend line over Africa.

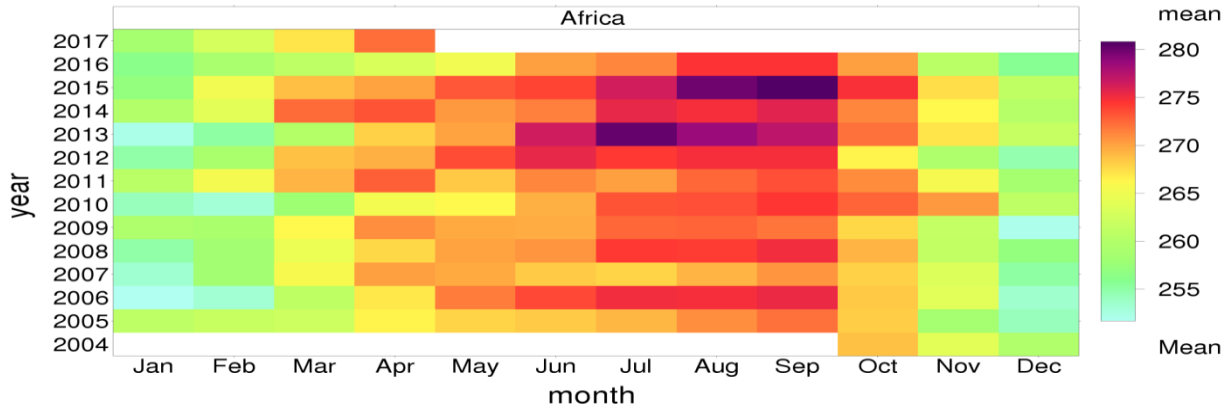

Figure 6: Heat map of Monthly means of TCO over Africa.

3.2.2 Antarctica

Antarctica is commonly called cold and white continent, in which the TCO has a positive trend of 0.957 DU/year (Figure 8). The spatial Climatological map shows low TCO over Eastern Antarctica as compared with the Western Antarctica. The lower values of TCO observed in the September and October months. This large variation in the TCO due to the atmospheric chemistry occurred in the early spring time in September to November months. This ozone depletion is high in the western Antarctica as compared to the Eastern Antarctica (Figure 7). High concentrations of TCO are identified in the June, July months and the least values are found in the ozone depletion period (Figure 9).

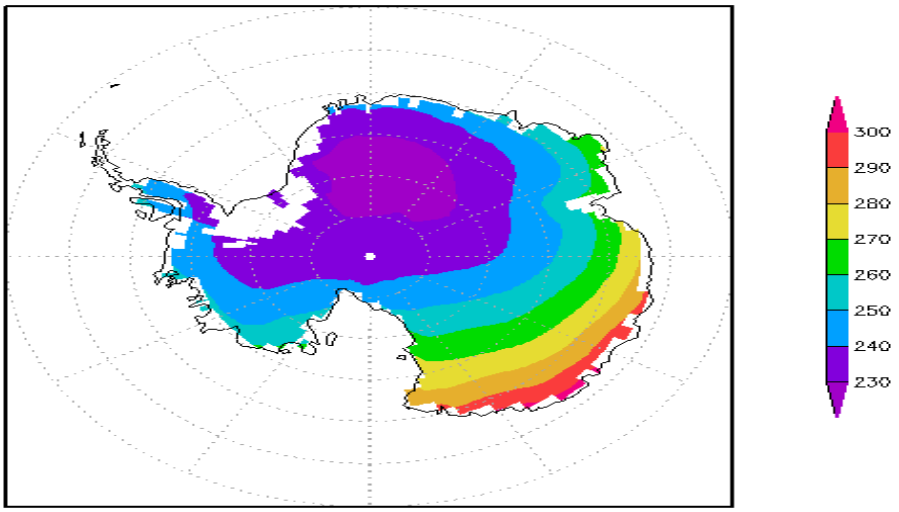

Figure 7: Climatology of TCO over Antarctica (2004-2017).

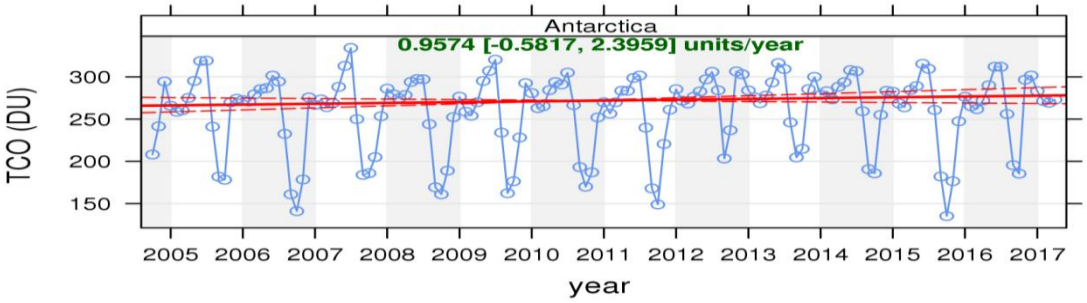

Figure 8: Mean TCO Theilsen trend line over Antarctica.

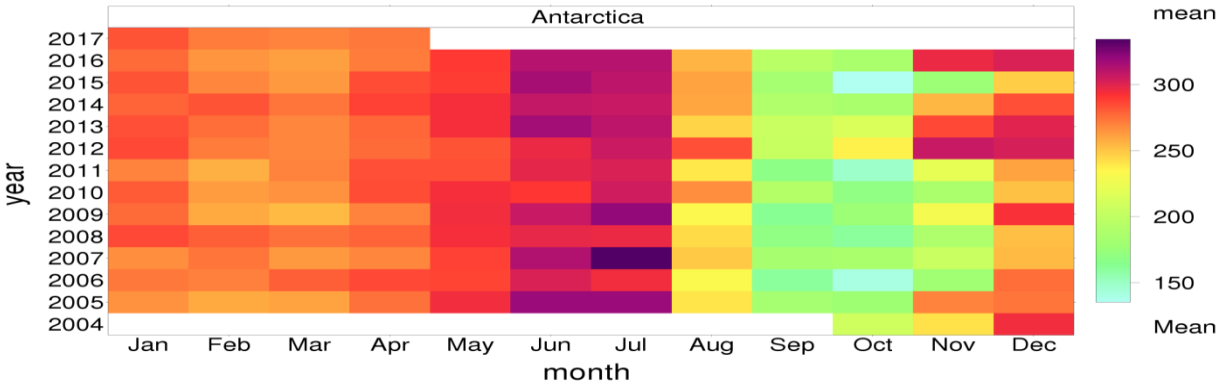

Figure 9: Heat map of Monthly means of TCO over Antarctica.

3.2.3 Asia

Asia is a largest continent in the world, here the TCO has a positive trend of 0.681 DU/year. Highest TCO concentrations are found in the North-Eastern parts of Asia and the lowest TCO values are found in the lower latitudes of Asia. Asia continent receives highest TCO concentrations in February, March, April and May months (Figure 11). A positive trend of ozone layer is noticed by 0.681 DU/year during the study period.

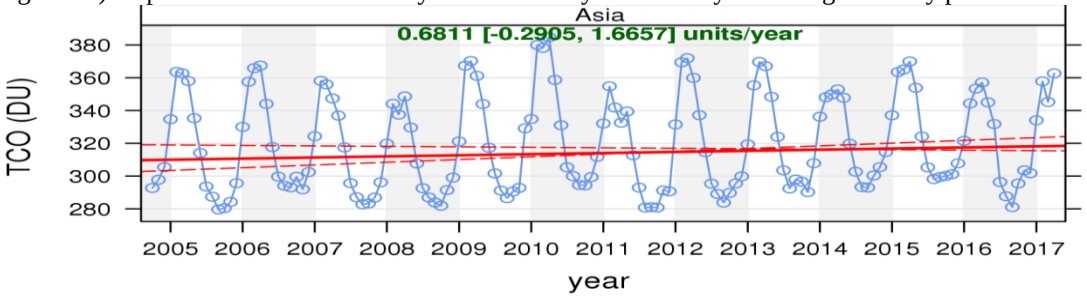

Figure 10: Mean TCO Theilsen trend line over Asia.

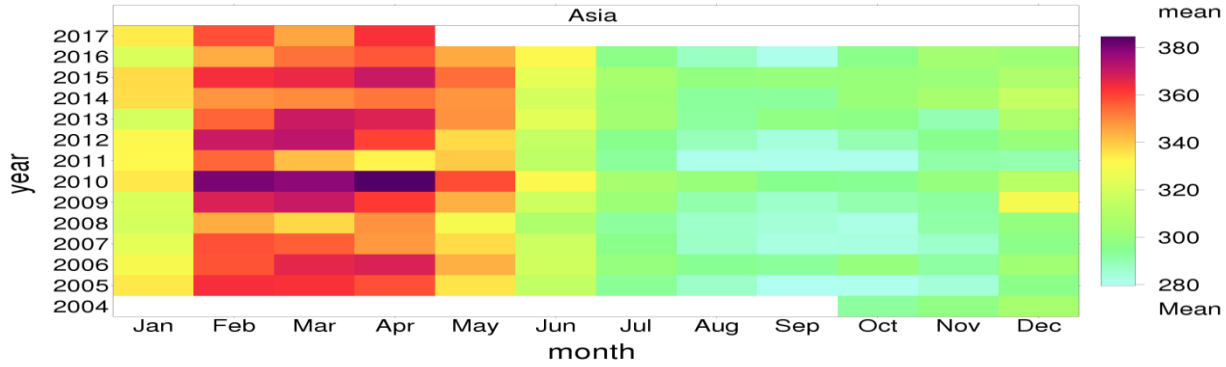

Figure 11: Heat map of Monthly means of TCO over Asia.

3.2.4 Australia

The spatial Climatological mean values shows high concentration of TCO in the Southern parts of Australia and low concentrations are at Northern parts of Australia (Figure 3). There is no significant trend is noticed during the study period, but it shows a positive trend of 0.071 DU/year over Australia. High TCO concentrations are found in the September, October months and the low values are found in the January, February, March and April months.

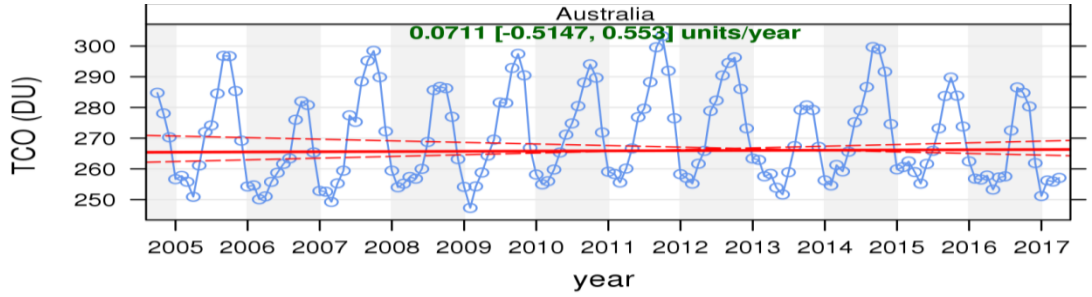

Figure 12: Mean TCO Theilsen trend line over Australia.

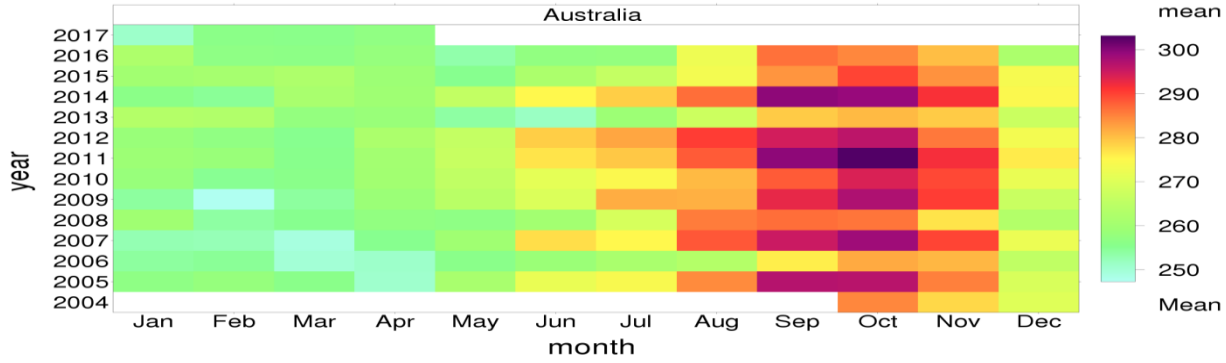

Figure 13: Heat map of Monthly means of TCO over Australia.

3.2.5 Europe

A significant positive trend of 0.342 DU/year is noticed over Europe. The high TCO concentrations are found in the February, March and April months and the lowest TCO concentrations are found in the October, November months. Spain, Portugal countries are having lowest TCO among the European countries. These TCO concentrations are increasing with respect to the latitude.

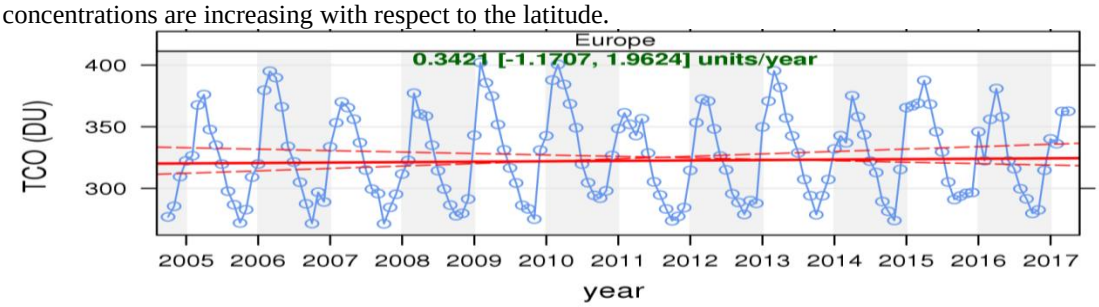

Figure 14: Mean TCO Theilsen trend line over Europe.

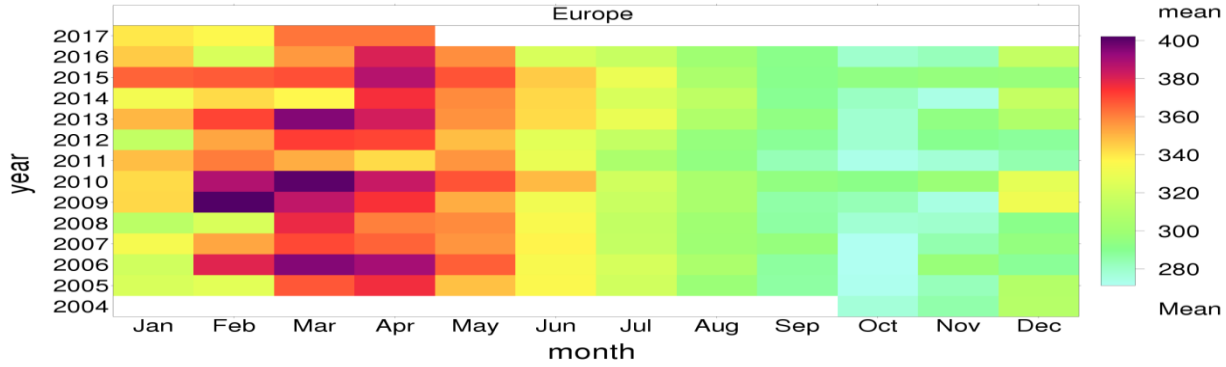

Figure 15: Heat map of Monthly means of TCO over Europe.

3.2.6 North America:

Low concentrations of TCO are found in the lower latitudes and high TCO concentrations are found in the higher latitudes. A positive trend of 0.83 DU/year has been noticed over the North American region and highest TCO concentrations are found in the March, April months and lowest values in September, October months.

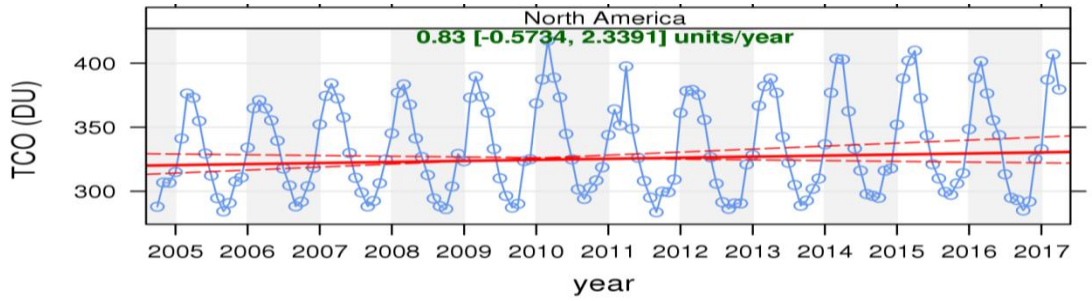

Figure 16: Mean TCO Theilsen trend line over North-America.

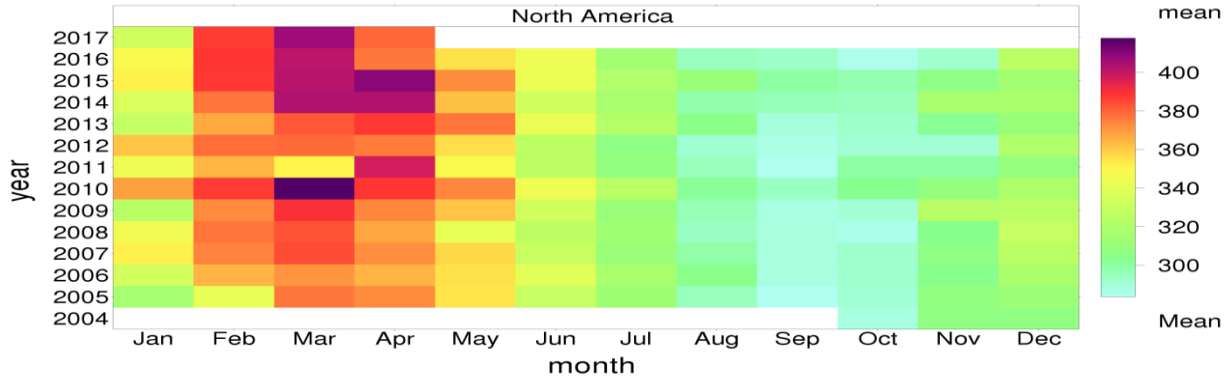

Figure 17: Heat map of Monthly means of TCO over North-America.

3.2.7 South America

Climatologal mean of South America shows the low TCO concentration at West part as compared to the Eastern part of the continent. And high TCO concentrations are found at the Southern part of the continent. A positive trend of 0.374 DU/year has been noticed over the South American region. High TCO concentrations are found in the August, September and October months where as the lowest values are found in February, March and April months.

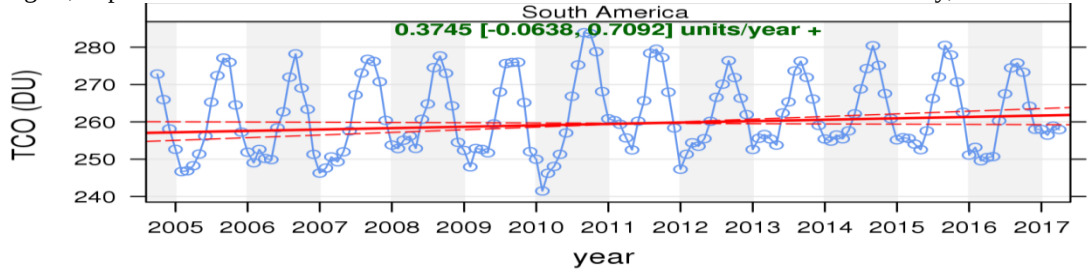

Figure 18: Mean TCO Theilsen trend line over South-America.

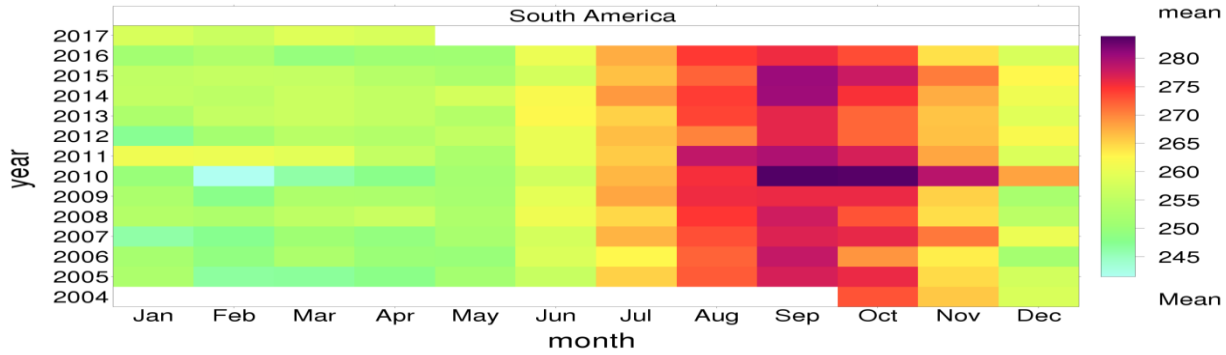

Figure 19: Heat map of Monthly means of TCO over South-America.

3.2.8 Northern and Southern Hemisphere:

Northern hemisphere, southern hemisphere both TCO concentrations are in positive trend by 0.499, 0.383 DU/year. There is high depletion of TCO occurred in 2006 and 2015 (Figure 20, 21). Figure 22, 23 shows the TCO concentration is directly proportional to the sun light intensity, where the sun light intensity is high in the March to May in Northern hemisphere and September to November in Southern hemisphere.

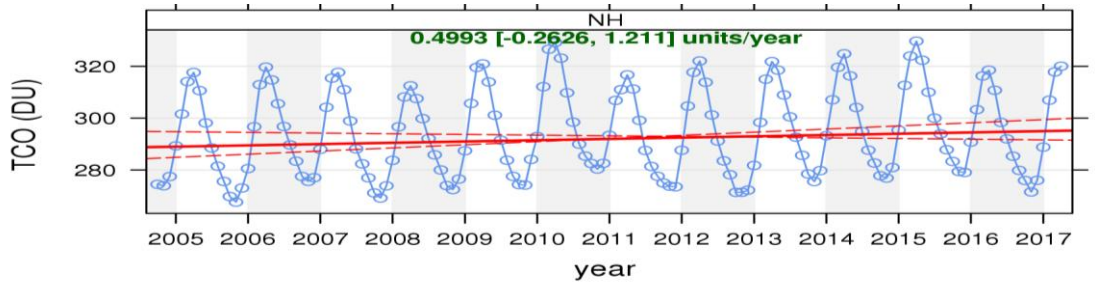

Figure 20: Mean TCO Theilsen trend line over South- Hemisphere.

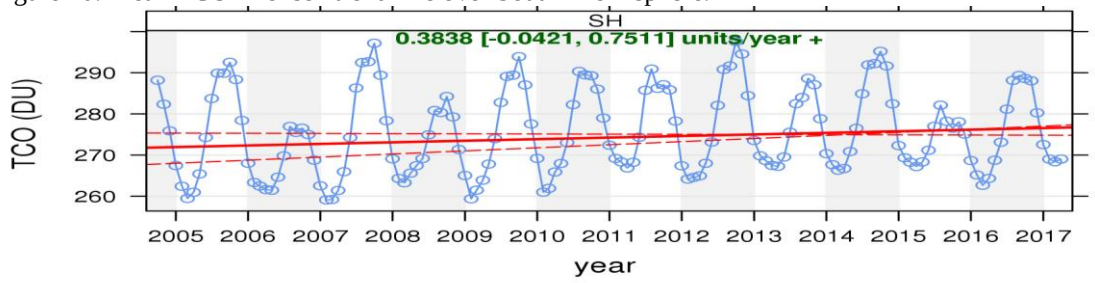

Figure 21: Mean TCO Theilsen trend line over South-Hemisphere.

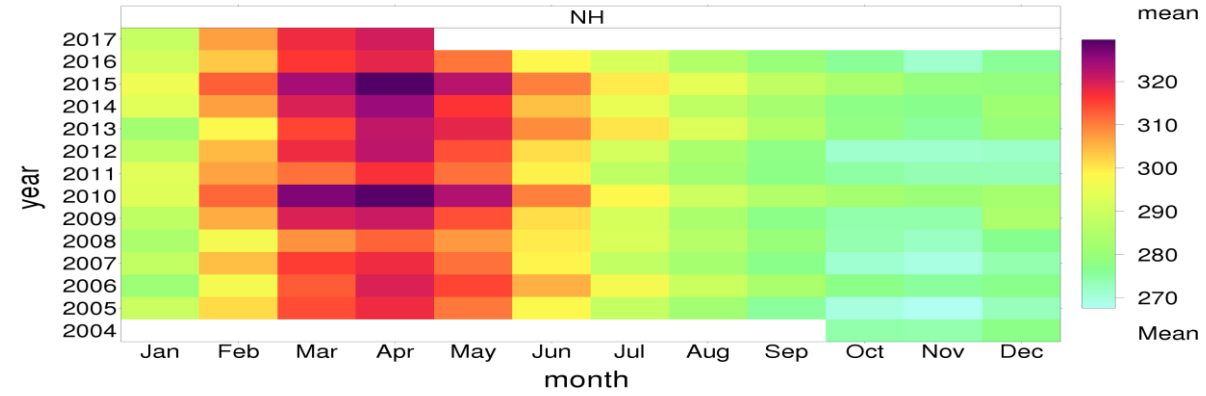

Figure 22: Heat map of Monthly means of TCO over Northern Hemisphere.

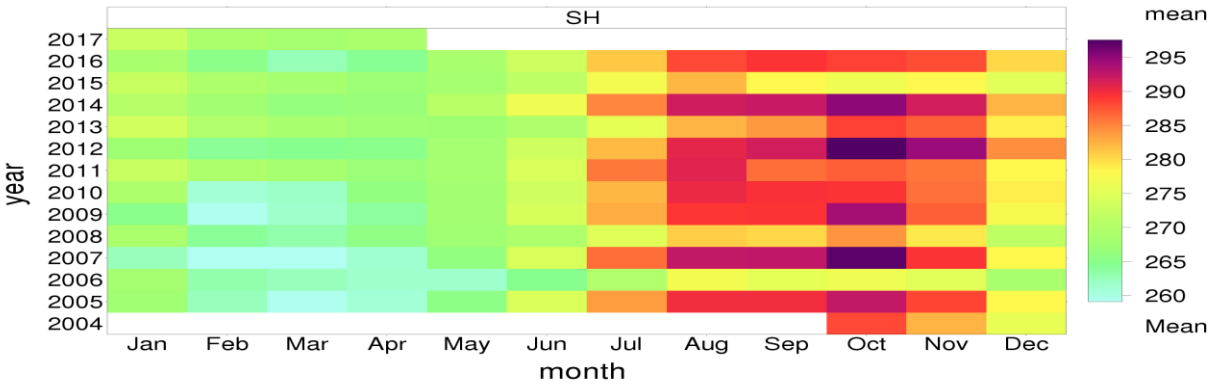

Figure 23: Heat map of Monthly means of TCO over Southern Hemisphere.

4 Conclusion

TCO formation is found high in the northern hemisphere as compared to the southern hemisphere. The continental trend line shows the increasing of TCO over the all parts of globe. This increasing trend is high in the northern hemisphere as 0.83 DU/year in North America and 0.68 DU/year in Asian region. Australia has a weak positive trend over the study period. The depletion of Ozone layer in the stratosphere is high in the winter seasons and low in the summer seasons. The monthly minimum values are noticed in the winter season months of both northern and southern hemisphere and high values are noticed in the summer periods of both northern and southern hemisphere. Antarctica ozone hole period is high in the 2006, 2015 year in the end of the winter months and its recovery also done is next followed months.

Acknowledgement: The authors are thankful to NASA for providing the OMI satellite data and also Director General of Meteorology of India Meteorological Department for encouraging this work.

References:

Balis, D., Kroon, M., Koukouli, M.E., Brinksma, E.J., Labow, G., Veefkind, J.P., McPeters, R.D., 2007. Validation of Ozone Monitoring Instrument total ozone column measurements using Brewer and Dobson spectrophotometer ground-based observations. J. Geophys. Res. Atmos. 112, 1–10. doi:10.1029/2007JD008796

Farman, J.C., Gardiner, B.G., Shanklin, J.D., 1985. Large losses of total ozone in Antarctica reveal seasonal ClO x /NO x interaction. Nature 315, 207–210. doi:10.1038/315207a0

Giannini, S.H., 1986. EFFECTS OF CHANGES IN STRATOSPHERIC OZONE AND GLOBAL CLIMATE.

Herman, J., Evans, R., Cede, A., Abuhassan, N., Petropavlovskikh, I., McConville, G., 2015. Comparison of ozone retrievals from the Pandora spectrometer system and Dobson spectrophotometer in Boulder, Colorado. Atmos. Meas. Tech. 8, 3407–3418. doi:10.5194/amt-8-3407-2015

James, G., T., 1986. Effects of Changes in Stratospheric Ozone and Global Climate: Sea level rise.

Kuttippurath, J., Lefèvre, F., Roscoe, H.K., Goutail, F., Pazmiño, A., Shanklin, J.D., 2013. Antarctic ozone loss in 1979-2010: First sign of ozone recovery. Atmos. Chem. Phys. 13, 1625–1635. doi:10.5194/acp-13-1625-2013

Levelt, P., Joiner, J., Tamminen, J., Veefkind, P., Bhartia, P.K., Stein Zweers, D., Duncan, B.N., Streets, D.G., Eskes, H., van der A, R., McLinden, C., Fioletov, V., Carn, S., de Laat, J., DeLand, M., Marchenko, S., McPeters, R., Ziemke, J., Fu, D., Liu, X., Pickering, K., Apituley, A., Gonzáles Abad, G., Arola, A., Boersma, F., Chan Miller, C., Chance, K., de Graaf, M., Hakkarainen, J., Hassinen, S., Ialongo, I., Kleipool, Q., Krotkov, N., Li, C., Lamsal, L., Newman, P., Nowlan, C., Suileiman, R., Tilstra, L.G., Torres, O., Wang, H., Wargan, K., 2017. The Ozone Monitoring Instrument: Overview of twelve years in space. Atmos. Chem. Phys. Discuss. 1–61. doi:10.5194/acp-2017-487

Levelt, P.F., Hilsenrath, E., Leppelmeier, G.W., Oord, G.H.J. Van Den, Bhartia, P.K., Tamminen, J., Haan, J.F. De, Veefkind, J.P., 2006. Science Objectives of the Ozone Monitoring Instrument. IEEE Geosci. Remote Sens. Lett. 44, 1199–1208.

Liu, X., Bhartia, P.K., Chance, K., Spurr, R.J.D., Kurosu, T.P., 2010. Ozone profile retrievals from the Ozone Monitoring Instrument. Atmos. Chem. Phys. Atmos. Chem. Phys. 10, 2521–2537. doi:10.5194/acpd-9-22693-2009

McPeters, R.D., Frith, S., Labow, G.J., 2015. OMI total column ozone: Extending the long-term data record. Atmos. Meas. Tech. 8, 4845–4850. doi:10.5194/amt-8-4845-2015

Nash, E.R., Newman, P.A., Rosenfield, J.E., Schoeberl, M.R., 1996. An objective determination of the polar vortex using Ertel's potential vorticity. J. Geophys. Res. 101, 9471–9478. doi:10.1029/96JD00066

Norval, M., Cullen, A.P., de Gruijl, F.R., Longstreth, J., Takizawa, Y., Lucas, R.M., Noonan, F.P., van der Leun, J.C., 2007. The effects on human health from stratospheric ozone depletion and its interactions with climate change. Photochem. Photobiol. Sci. 6, 232. doi:10.1039/b700018a

Proffitt, M.H., Margitan, J.J., Kelly, K.K., Loewenstein, M., Podolske, J.R., Chan, K.R., 1990. Ozone loss in the Arctic polar vortex inferred from high-altitude aircraft measurements. Nature 347, 31–36. doi:10.1038/347031a0

Schoeberl, M.R., Hartmann, D.L., 1991. The dynamics of the stratospheric polar vortex and its relation to springtime ozone depletions. Science 251, 46–52. doi:10.1126/science.251.4989.46

Sen, P.K., 1968. Estimates of the Regression Coefficient Based on Kendall's Tau. J. Am. Stat. Assoc. 63, 1379. doi:10.2307/2285891

Soni, V.K., Sateesh, M., Das, A.K., Peshin, S.K., 2017. Progress in Meteorological Studies around Indian Stations in Antarctica. Proc. Indian Natl. Sci. Acad. 90, 461–467. doi:10.16943/ptinsa/2017/48954

Stolarski, R.S., Krueger, A.J., Schoeberl, M.R., McPeters, R.D., Newman, P.A., Alpert, J.C., 1986. Nimbus 7 satellite measurements of the springtime Antarctic ozone decrease. Nature 322, 808–811. doi:10.1038/322808a0

Theil, H., 1950. A rank-invariant method of linear and polynomial regression analysis. I. Nederl. Akad. Wetensch., Proc. 53, 386–392. doi:10.1007/978-94-011-2546-8

Vaz Peres, L., Bencherif, H., Mbatha, N., Schuch, A.P., Mohamed Toihir, A., Bègue, N., Portafaix, T., Anabor, V., Kirsch Pinheiro, D., Maria Paes Leme, N., Bageston, J.V., Jorge Schuch, N., 2017. Measurements of the total ozone column using a Brewer spectrophotometer and TOMS and OMI satellite instruments over the Southern Space Observatory in Brazil. Ann. Geophys. 35, 25–37. doi:10.5194/angeo-35-25-2017

Veefkind, J.P., Bhartia, P.K., Gleason, J., de Haan, J.F., Wellemeyer, C., Qin, W., Levelt, P.F., 2003. Total Ozone from the Ozone Monitoring Instrument (OMI) using TOMS and DOAS Methods. EGS - AGU - EUG Jt. Assem. 44, 8932. doi:10.1109/TGRS.2006.871204

Waugh, D.W., 1993. Subtropical stratospheric mixing linked to disturbances in the polar vortices. Nature 365, 535–537. doi:10.1038/365535a0